CONFERENCE PRE-PRINT

ELM CONTROL BY 3D MAGNETIC PERTURBATIONS IN HL-3/HL-2A TOKAMAKS

G.Z. Hao Southwestern Institute of Physics Chengdu, China Email: haogz2019@outlook.com

L. Wang Southwestern Institute of Physics Chengdu, China

J. Huang Southwestern Institute of Physics Chengdu, China

Y.Q. Liu General Atomics San Diego, USA

M. Becoulet CEA Saint-Paul-Lez-Durance, France

T.F. Sun Southwestern Institute of Physics Chengdu, China

N. Zhang Southwestern Institute of Physics Chengdu, China

G.Q. Dong Southwestern Institute of Physics Chengdu, China

Abstract

Externally applied Resonant Magnetic Perturbation (RMP) has been proven as an effective approach for edge localized mode (ELM) control. The paper reports recent progress of ELM control with RMP on the HL-3/HL-2A tokamaks. The three-dimensional (3D) magnetohydrodynamic (MHD) code JOREK was utilized to perform both linear and nonlinear studies for HL-2A. The linear modeling results revealed that the formation of the periodic structure of equilibrium generated by RMPs is the mechanism for the transition of the dominant toroidal mode number of ELM. On the other hand, the nonlinear modeling results indicate that the mode coupling plays the key role in mitigating ELMs. A series of nonlinear modeling starting at different equilibriums with varied q-profile reveals that the alignment of magnetic islands generated at rational surfaces and the pedestal top could provide extra transport to limit the height and width of pedestal thus keep the pedestal from entering peeling-ballooning unstable regions, which serves as one candidate for the explanation of RMP induced ELM suppression. Preliminary modeling studies have also been done for the HL-3 tokamak, which well recovers the experimental observed phenomenon.

1. INTRODUCTION

Transient events such as edge localized modes (ELMs) have become a major concern for future tokamaks operating under high confinement mode (H-mode) [1] due to their capability of releasing large amount of energy to plasma facing components [2-3]. Resonant magnetic perturbations (RMPs) have been experimentally demonstrated as an effective approach to either mitigate [4-6] of totally suppress ELMs [7-9], but the underlying mechanism remain unclear. Since ELMs are believed to be governed by coupled peeling-ballooning modes [10-11], RMP induced ELM control can be intuitively understood from the perspective that the interaction between

RMP and ELM has changed the stability conditions for peeling-ballooning modes. Still, more sophisticated studies await.

The paper uses the three-dimensional (3D) nonlinear magnetohydrodynamic code JOREK to perform both linear and nonlinear studies on RMP induced ELM control for the HL-2A and HL-3 tokamak. The experimental data from shot 36872 is used for the study of HL-2A, and the nonlinear modeling results reproduce most of the experimental observations. Moreover, by carefully examining the plasma response to the applied RMP field and analyzing time evolution of the plasma edge profiles, the physics involved in the nonlinear interaction between the plasma and RMP during ELM mitigation is further clarified. While the equilibrium based on experimental data cannot reach ELM suppression regime even with a sufficiently large RMP coil current, by adjusting the equilibrium with different q-profile, ELM suppression is successfully realized in the modeling. On the other hand, linear studies have also been performed to investigate the dominant mode transition during application of RMP as well as the modification of 3D equilibrium caused by externally applied perturbation fields. For the HL-3 tokamak, the data from shot 6545 is used as input for JOREK, where ELM mitigation regime is reached when RMP is applied. Preliminary modeling results recovers most of the experimental observation, while more detailed modeling needs to be done in future works.

The paper is organized as follows. Section 2 will introduce the modeling results for ELM mitigation on HL-2A, and the ELM suppression results will be given in Section 3. Section 4 shows the preliminary results for HL-3. Section 5 summarizes the paper with conclusions.

2. ELM MITIGATION MODELING ON HL-2A

The HL-2A tokamak has a major radius of R=1.65 m, minor radius of $\alpha=0.4$ m, and toroidal field of $B_T=1.0-1.3$ T. There are two set of RMP coils installed on HL-2A, toroidally seperated by 180 degrees, with each set consisting of 2 coils mounted symmetrically above and below the mid-plane. In shot 36872, type-I ELMs were present after the plasma enters H-mode. The RMP was applied at t=1400 ms and lasted for 50 ms with odd parity, meaning there was a phase difference of 180 degrees between the top and bottom rows of coils. ELMs were successfully mitigated after about 20 ms the switch-on of RMP with a coil current of 4.9 kAt, as shown in Fig. 1 left panel (a)-(e). Based on experimental measured diagnostics data, JOREK successfully modeled the natural ELMs [12], as shown in Fig.1 right panel solid lines. To simulate mitigated ELMs, the n=1 RMP is frst applied to the two-dimensional (2D) equilibrium at $t\sim0.4$ ms to evolve until stationary, where a new 3D equilibrium is reached, then other harmonics are initialized at $t\sim0.85$ ms to evolve self-consistently. As can be seen in Fig.1 right panel dashed lines, the maximum magnetic energy for the most unstable mode decreased substantially, implying that ELMs were successfully mitigated.

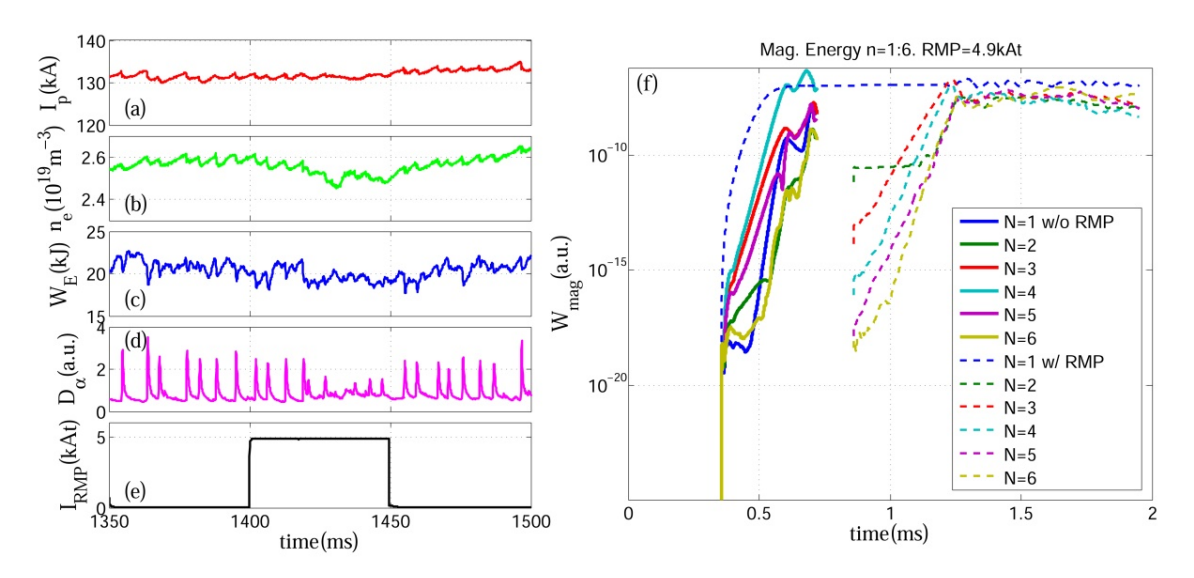


FIG. 1. Left Panel: Time traces of discharge parameters in shot 36872, showing (a) the plasma current, (b) the electron density, (c) the plasma stored energy, (d) the D_{α} signal and (e) the ELM control coil current, respectively. Right Panel: The JOREK simulated magnetic energy evolution of the toroidal modes n=1-6 over time, for both the natural (solid lines) and the mitigated (dashed lines) ELMs with the n=1 RMP at

 $I_{RMP} = 4.9$ kAt. For the latter case, the n = 1 RMP is frst applied at $t \sim 0.4$ ms to evolve until stationary, then other harmonics are initialized at $t \sim 0.85$ ms [12].

The current requirement for the RMP coils is critical for achieving ELM control, which can only be quantified with nonlinear modeling. A systematic scan of RMP coil current has been perform to quantitatively predict the coil current threshold needed to reach ELM mitigation. The scan starts from the same 2D equilibrium established based on experimental inputs, following the same procedure as mentioned above, where different coil currents are assumed to first generate a series of 3D equilibrium, then other harmonics are added to self-consistently evolve until saturation. Fig. 2 shows magnetic energies for all modes at the time when the most unstable toroidal mode reaches the maximum value (this time may be different for each case), with the coil current varying from 1.0 kAt to 7.5 kAt [12]. Shown is also the pure ELM case (with zero coil current) for comparison. With the increase of coil current, the most unstable mode changes from n = 4 to n = 3 mode, while its magnitude stays almost unaffected until the coil current reaches 4.5 kAt, where a substantial magnetic energy reduction of the most unstable mode is observed. Thus, a coil current threshold value of about 4.5 kAt can be inferred. Note that the most unstable mode changes from n = 4 to n = 3 mode when the RMP coil current reaches 4 kAt, presumably arising from a stronger coupling effect of the n = 3 mode to the applied n = 1 RMP.

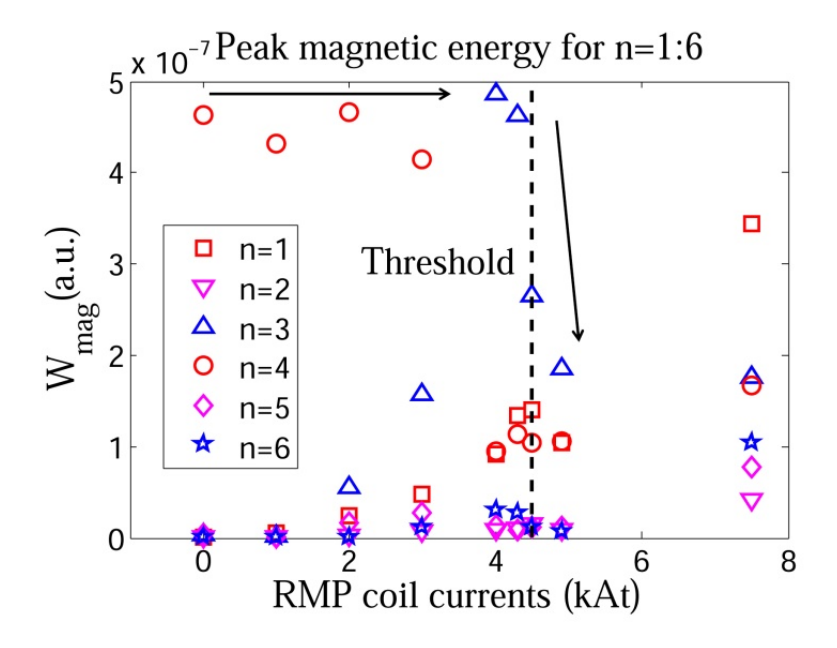


FIG. 2. Magnetic energies for all modes at the time when the most unstable toroidal mode reaches the maximum value. The case with no RMP corresponds to zero coil current. The dashed line shows the inferred RMP coil current needed for ELM mitigation. Black arrows are guides to the eye [12].

To further check the transition of dominant toroidal modes, a series of linear scans have been performed with different RMP coil currents. Here, the linear study means that the n=0 component is fixed in the simulation. The primary objective of this investigation was to gain insights into how RMP affects plasma 3D equilibrium and, consequently, the transition of dominant toroidal modes. To better illustrate the 3D weak equilibrium, the density perturbations along the toroidal (ϕ) and poloidal (θ) directions have been extracted to create 2D plots for all cases, as shown in Fig. 3 [13]. The data used here is chosen at $1000\tau_A$ after the introduction of higher-n harmonics. Without losing generality, the radial positions shown in Fig. 3 are (a-e) $\psi_n = 0.6$ (f-j) $\psi_n = 0.8$, and (k-o) $\psi_n = 0.95$, corresponding to safety factors of q=2, 3, and 4, respectively. In the poloidal direction, $\theta = 0$ (π) denotes the mid-plane at the low (high) field side. By scanning the RMP coil current, it is observed that an increase in RMP coil current makes the n=1 periodic structure more pronounced, which is even more evident at the outer radial position ($\psi_n = 0.95$), since RMP has a greater influence on plasma edge than core. From Fig. 3 (k-o), it is obvious that when the RMP coil current is less than 3 kAt, the dominant toroidal mode number is n=4. As the current increases, the dominant mode shifts to n=3. This indicates that the introduction of RMP significantly affects plasma equilibrium, which in turn influences the instability itself and causes the dominant toroidal mode to change.

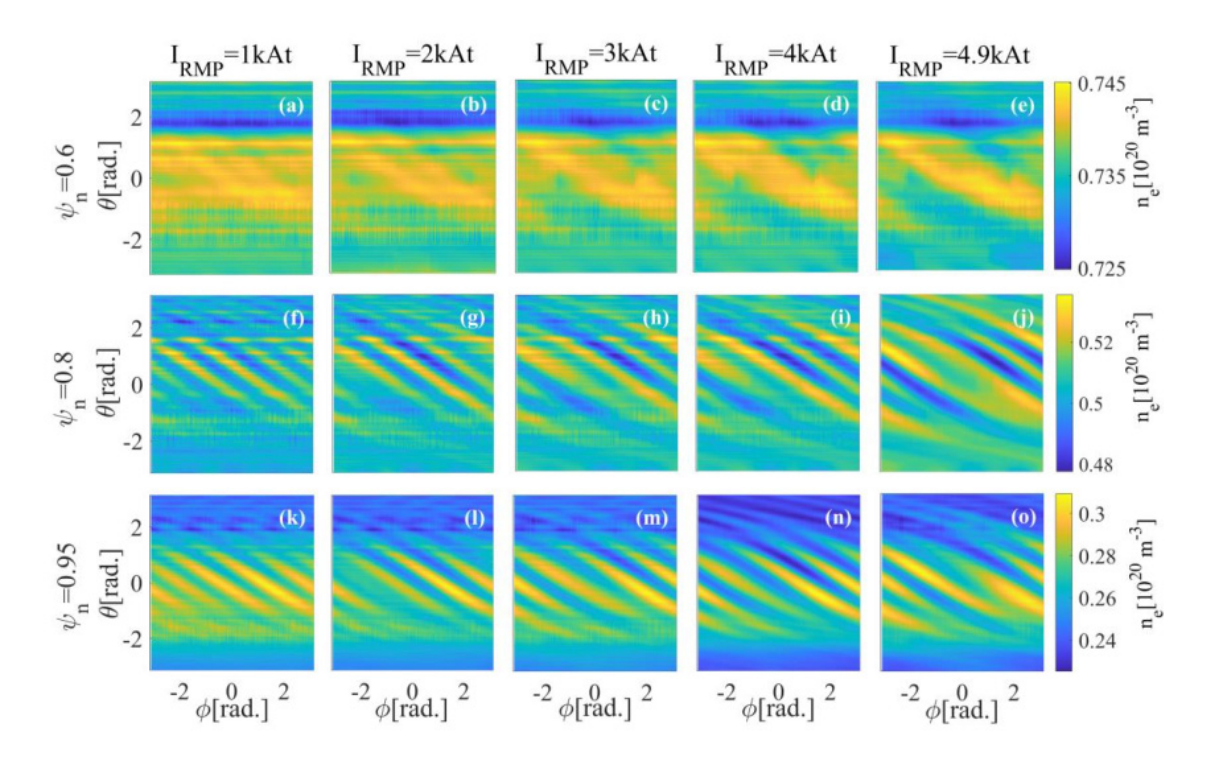


FIG. 3. The 2D plot of density perturbations along the toroidal (ϕ) and poloidal (θ) angles, at different radial locations: (a-e) $\psi_n = 0.6$, (f-j) $\psi_n = 0.8$, and (k-o) $\psi_n = 0.95$. Considered are also different RMP coil currents: 1, 2, 3, 4, and 4.9 kAt, respectively. All the n = 0 - 6 toroidal components are included in the JOREK simulations. Compared are the results at the simulation time $1000\tau_A$ after the introduction of higher-n harmonics [13].

3. ELM SUPPRESSION MODELING ON HL-2A

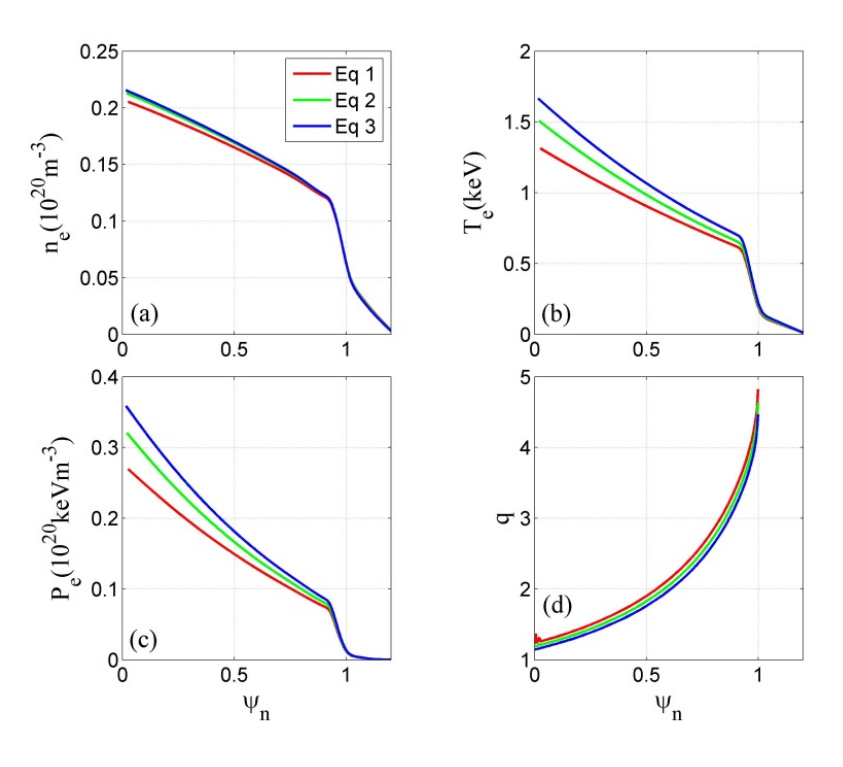


FIG. 4. The equilibria with flows reconstructed using JOREK, showing radial profiles at the mid-plane of (a) the electron density, (b) the electron temperature, (c) the electron pressure and (d) the safety factor.

It is worthwhile mentioning that after achieving ELM mitigation, further increase of the RMP coil current can potentially leads to ELM suppression. In Fig. 2, however, no complete ELM suppression is observed even after increasing the coil current to 7.5kAt. Since no ELM suppression has been achieved on HL-2A (up to the coil current design limit), the modeling results are consistent with the experiment. Moreover, this emphasizes the vital role played by the plasma configuration for achieving ELM suppression. In order to model ELM suppression in JOREK, the original 2D equilibrium is modified to generate 3 new ones by adjusting the initial input profiles. The new equilibria are displayed in Fig. 4, referred as Eq 1, Eq 2 and Eq 3, respectively. These equilibria have almost identical density profiles, while the temperature profiles and q-profiles differ a lot. Note that though the pedestal height is different for each equilibrium, the radial location of pedestal stays unchanged. Based on these equilibria, mitigated or suppressed ELMs are simulated in JOREK with application of 4.9 kAt RMPs, as presented in Fig. 5. The behaviour of ELMs is quite different for these cases. Despite the fact Eq 3 has the highest pedestal height, this case is the only one that reaches ELM suppression regime.

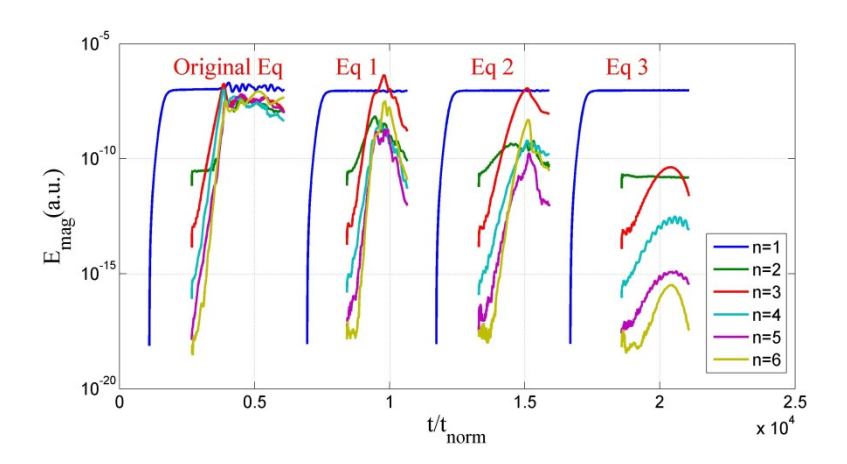


FIG. 5. The JOREK simulated magnetic energy evolution of the toroidal modes n=1-6 over time starting from different equilibria. For better visualization, each case is shifted horizontally correspondingly. The case starting from the original equilibrium is also repeated here for better comparison.

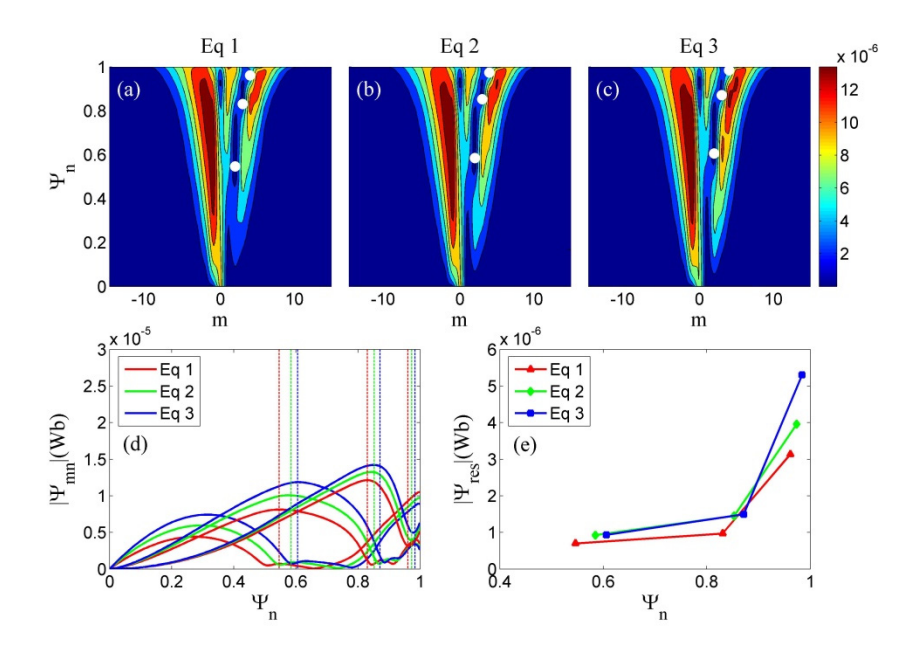


FIG. 6. The n=1 Fourier spectra of the poloidal magnetic flux for three cases with 4.9 kAt RMP coil current. (a-c) show the poloidal spectra for cases starting from Eq 1, Eq2 and Eq 3, respectively. (c) radial profiles of all resonant poloidal harmonics, and (d) magnitude of the resonant Fourier components at the corresponding rational surfaces. The white solid dots in (a-c) show the position of all resonant poloidal harmonics (n=1, m=2-4), with radial locations of the corresponding rational surfaces also indicated by vertical dashed lines in (d).

To investigate the possible mechanism that underlying ELM suppression, the plasma response to the applied RMP field is calculated. When the n=1 harmonic is added to the 2D axisymmetric equilibrium, the applied RMP field interacts with the plasma and slowly modifies the edge magnetic topology, resulting in a 3D equilibrium. Fig. 6 shows the n=1 Fourier spectra of the modeled poloidal magnetic flux for all the three cases with the n=1 RMP at $I_{RMP}=4.9$ kAt. Plot (a-c) here show the spectra for cases starting from Eq 1, Eq 2 and Eq 3, respectively. Due to the presence of plasma flow, these spectra show pronounced plasma screening of resonant harmonics near corresponding rational surfaces q=m/n indicated by white dots. Since the q-profile for each case is different, the location of white dots also differs. The screening is however not perfect with finite plasma resistivity. This is illustrated by Fig. 7(d) which plots the radial profiles of all resonant poloidal harmonics, as well as Fig. 7(e) showing the magnitude of the resonant Fourier components at corresponding rational surfaces. The screening is weaker near the plasma edge because of larger resistivity resulting from lower electron temperature. A stronger plasma response is developed for the case starting from Eq 3. In other words, the applied RMP in this case seems to be more efficient than other cases.

Since plasma screening of the penetrated resonant harmonics is only partial, it is possible for magnetic islands to be generated on corresponding rational surfaces. Fig. 7 shows the Poincare plots from the magnetic field line tracing for all cases. The magnetic islands are mainly generated near rational surfaces, such as the q = 2/1, q = 3/1, and q = 4/1 surfaces. Due to the q-profile change, the rational surfaces move outwards from case Eq 1 to case Eq 3, and consequently the q = 3/1 surface gets closer to pedestal top. On the other hand, there is no q = 4/1 magnetic islands in the case starting from Eq 3, since the q = 4/1 surface is too close to the separatrix. Instead, a stochastic layer formed in this region. The change of the magnetic topology can then tailor characteristics of the edge radial transport and consequently evolution of the edge profiles, especially the magnetic islands formed on pedestal top, which is capable of limiting the height of the pedestal. Indeed, the profile evolution for case Eq 3 presented in Fig. 8 shows a constant decreasing of pedestal height, which explains the onset for ELM suppression of this case [14].

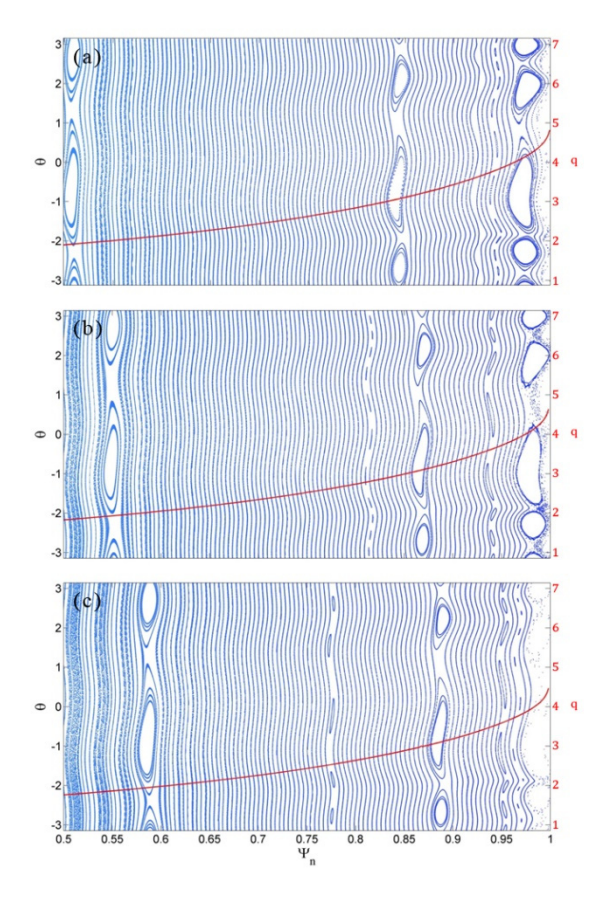


FIG. 7. Poincare plots of the magnetic field lines near the plasma edge for the simulated cases with 4.9kAt RMP coil current, showing the magnetic topology for cases starting from (a) Eq 1, (b) Eq 2, and (c) Eq 3, respectively. The red curve in each plot shows the q-profile for each case.

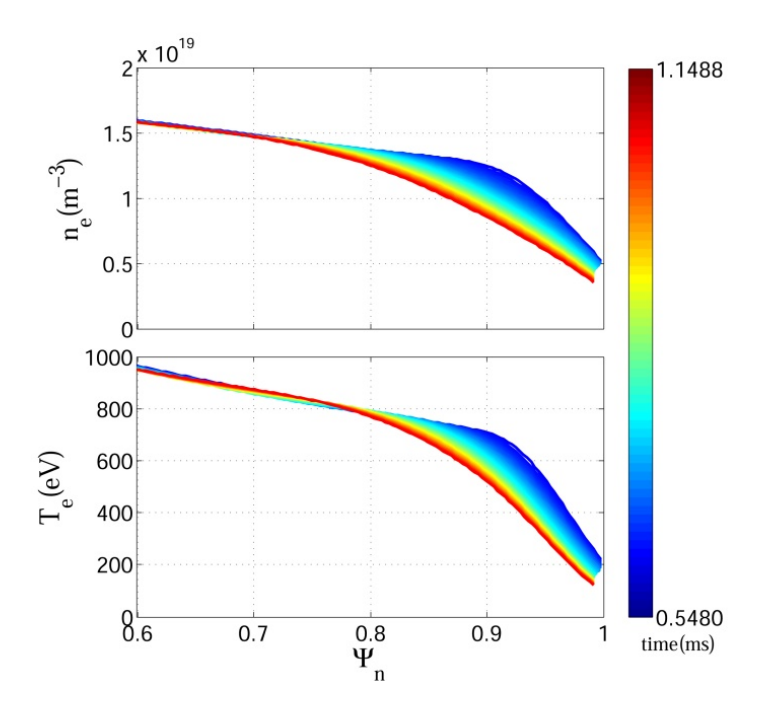


FIG. 8. Flux-surface averaged radial profiles of (a) the electron density, and (b) the electron temperature of the simulated ELM suppression case (Eq 3) with 4.9 kAt RMP coil current.

4. ELM MITIGATION MODELING ON HL-3

Only preliminary results will be given in the section. The main parameters for the HL-3 tokamak are: major radius R = 1.78 m, minor radius a = 0.65 m, and toroidal field $B_T = 1.5 - 2.3$ T. There are eight set of RMP coils installed on HL-3, with each coil toroidally covering 36 degrees and poloidally 17 degrees. The configuration of RMP coils is capable of generating perturbation fields with toroidal mode number up to n = 4. In shot 6545, the RMP was applied at t = 1400 ms, when type-I ELMs were present after the plasma enters H-mode. The ELMs were successfully mitigated for about $20 \sim 30$ ms before an H-L back-transition happened, as shown in Fig. 9 left panel. Based on experimental data, nonlinear modeling for both the natural and mitigated ELMs are performed using JOREK, as shown in Fig.9 right panel.

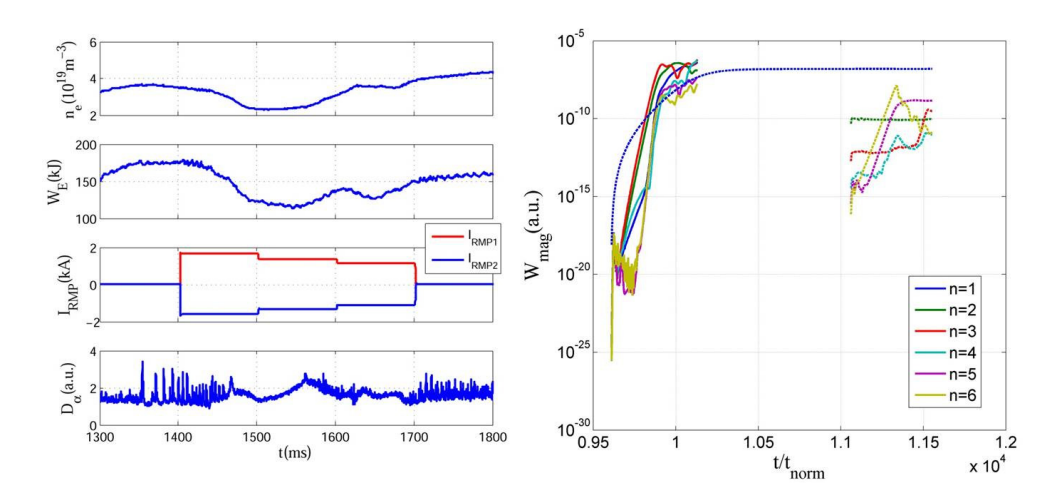


FIG. 9. Left Panel: Time traces of discharge parameters in shot 6545, showing (a) the plasma density, (b) the total stored energy, (c) the ELM control coil current, and (d) the D_{α} signal, respectively. Right Panel: The JOREK simulated magnetic energy evolution of the toroidal modes n=1-6 over time, for both the natural (solid lines) and the mitigated (dashed lines) ELMs with the n=1 RMP at $I_{RMP}=4.9$ kAt. For the latter case, the n=1 RMP is frst applied at $t\sim0.96$ ms to evolve until stationary, then other harmonics are initialized at $t\sim1.11$ ms.

It should be mentioned here that due to some numerical issues, the results of mitigated ELMs shown above are not very convincing. The modeling encountered severe numerical instability due to the emergence of negative density or temperature. To solve the problem, some techniques are used in the modeling, including adding additional density refection at the modeling boundary, setting negative density and temperature diffusive coefficients to correct negative density and temperature, using shock-capture mechanisms, etc. By doing so, the results are much less physical, but rather artificial. Nevertheless, a more detailed modeling will be conducted in future works.

5. CONCLUSIONS

Utilizing the nonlinear MHD code JOREK, we have simulated both the natural and the mitigated ELMs for the HL-2A tokamak assuming the experimental parameters. The modeling results agree well with experimental observations. By performing a series of JOREK nonlinear simulations with different RMP coil current amplitudes, a threshold value of about 4.5kAt to achieve ELM mitigation on HL-2A is identified, in agreement with the experimental observation. By also doing a scan of linear studies, the modeling results revealed that the formation of the periodic structure of equilibrium generated by RMPs is the mechanism for the transition of the dominant toroidal mode number of ELMs.

To simulate ELM suppression by RMP, three equilibria with different q-profiles were generated. The change of q-profile significantly influences the generation of magnetic islands such that good alignment of magnetic islands and pedestal top is reached for the case Eq 3. Consequently, extra transport is induced and the height of pedestal is limited to under the stability boundary of peeling-ballooning modes. This explains the mechanism which underlies the onset of RMP induced ELM suppression.

Last, preliminary studies have also been done for the HL-3 tokamak. Both the natural and the mitigated ELMs were successfully simulated with JOREK, consistent with experimental observations. However, due to numerical issues, no further simulation has been done yet, which will be left to future works.

ACKNOWLEDGEMENTS

This work is supported by the National Magnetic Confinement Fusion Energy R&D Program (No. 2022YFE03060002), the Youth Science and Technology Innovation Team of Sichuan Province (No. 2022JDTD0003), the National Natural Science Foundation of China with Grant No. 12375214, the China National Nuclear Corporation Fundamental Research Program (No. CNNC-JCYJ-202236), the Innovation Program of Southwestern Institute of Physics with Grant No.202301XWCX006-04, and the National Natural Science Foundation of China with Grant No. 12105082. This work is also supported by the US DoE Office of Science under Contracts DE-FG02-95ER54309 and DE-FC02-04ER54698.

REFERENCES

- [1] Wagner F. et al 1982 Phys. Rev. Lett. 49 1408
- [2] Zohm H. 1996 Plasma Phys. Control. Fusion 38 105
- [3] Kirk A., Wilson H.R., Counsell G.F., Akers R., Arends E., Cowley S.C., Dowling J., Lloyd B., Price M. and Walsh M. 2004 Phys. Rev. Lett. 92 245002
- [4] Kirk A. et al 2013 Nucl. Fusion 53 043007
- [5] Liang Y. et al 2007 Phys. Rev. Lett. 98 265004
- [6] Sun T.F., Liu Y., Ji X.Q., Liu Y.Q., Ke R., Gao J.M., Wu N., Deng W., Xu M. and Duan X.R. 2021 Nucl. Fusion 61 036020
- [7] Evans T.E. et al 2008 Nucl Fusion 48 024002
- [8] Suttrop W. et al 2018 Nucl. Fusion 58 096031
- [9] Jeon Y.M. et al 2012 Phys. Rev. Lett. 109 035004
- [10] Leonard A.W. 2014 Phys. Plasmas 21 090501
- [11] Snyder P.B., Wilson H.R. and Xu X.Q. 2005 Phys. Plasmas 12 056115
- [12] Wang L. et al 2024 Nucl. Fusion 64 096016
- [13] Liu Y.H.Z. et al 2025 Plasma Phys. Control. Fusion 67 055001
- [14] Hu Q.M. et al 2020 Phys. Rev. Lett. 125 045001